

- 1 **Supplementary Information**
- 2 **Table of contents**
- 3 **1. Materials**
- 4 **2. Preparation of Ru-MeCN complex**
- 5 **3. Fabrication of CC/p-RuCP by chemical polymerization of ruthenium complex**
- 6 **4. Preparation of IrO_x nanocolloid solution**
- 7 **5. Fabrication of SiGe-jn electrode**
- 8 **6. Fabrication of IrO_x/SiGe-jn photoanode**
- 9 **7. Fabrication of tablet-formed IrO_x/SiGe-jn/CC/p-RuCP device**
- 10 **8. Electrochemical/photoelectrochemical measurements**
- 11 **9. Calculation of the potential values versus RHE**
- 12 **10. Calculation of current efficiency for formate production**
- 13 **11. Current efficiency for formate production as a function of oxygen concentration in CO₂ flow**
- 14 **12. Current efficiency for formate production over RuCP coated onto the stainless steel surface of the**
15 **SiGe-jn photocathode or onto the CC connected with the SiGe-jn photocathode**
- 16 **13. Photodegradation of formate over IrO_x/SiGe-jn photoanode**
- 17 **14. CO₂ photoreduction reaction using tablet-formed IrO_x/SiGe-jn/CC/p-RuCP device**
- 18 **15. Determination of products in the aqueous phase**
- 19 **16. Determination of products in the gas phase**
- 20 **17. Calculation of solar-to-chemical conversion efficiency for formate production**

1 **18. References**

2 **Figure S1. Schematic illustration of SiGe-jn structure**

3 **Figure S2. Relation between applied potential and amount of formate generated over CC/p-RuCP**
4 **cathode**

5 **Table S1. Current efficiency for formate production over CC/p-RuCP cathode at various applied**
6 **potentials.**

7 **Table S2. Current efficiency for formate production with respect to the oxygen concentration in**
8 **CO₂ flow over SiGe-jn/CC/p-RuCP and InP/RuCP photocathodes under light irradiation**
9 **for 1 h in 0.1M phosphate buffer electrolyte.**

10 **Figure S3. Current-potential characteristics of CC and stainless steel substrates for SiGe-jn**

11 **Figure S4. Current-potential characteristics of CC under Ar or CO₂ atmospheres**

12 **Table S3. Current efficiency for formate production over RuCP coated onto the stainless steel**
13 **surface of the SiGe-jn photocathode or onto the CC connected with the SiGe-jn**
14 **photocathode**

15 **Figure S5. Amount of formate before and after photodegradation over the IrO_x/SiGe-jn photoanode**
16 **in various electrolytes.**

17 **Figure S6. Current-potential characteristics for the IrO_x/SiGe-jn photoanode**

18 **Figure S7. Current-potential characteristics for the IrO_x/ITO anode**

19 **Figure S8. Spectrum of simulated solar light**

1 **Figure S9. Current-potential characteristics for the IrO_x/SiGe-jn photoanode and CC/p-RuCP**
2 **cathode**

3 **Figure S10. Current-potential characteristics for the IrO_x/SiGe-jn photoanode and CC/p-RuCP**
4 **cathode in a two-electrode configuration under simulated solar light irradiation (1 sun,**
5 **AM1.5, 0.25 cm²)**

6 **Figure S11. Mass spectra of products observed in the CO₂ photoreduction reaction under ¹²CO₂ (A)**
7 **and ¹³CO₂ (B) atmospheres.**

8

1 **1. Materials**

2 Dipotassium hydrogen phosphate (Wako Pure Chemical Industries, Ltd.), potassium dihydrogen
3 phosphate (Kanto Chemical Co., Inc.), carbon dioxide gas (Taiyo Nippon Sanso), formic acid (88%, Kanto),
4 acetonitrile (MeCN: Kanto), pyrrole (Kanto), iron(III) chloride hexahydrate (99.9%, Wako), ethanol (Wako),
5 potassium hexachloroiridate(IV) (Wako), nitric acid (69 vol%, Wako), sodium hydroxide (Wako), iridium
6 metal plate (99.9%, Kojundo Chemical Laboratory Co., Ltd.), and indium tin oxide (ITO) etching solution
7 (ITO-07N, Kanto) were used as-received. Pure water (>18 MΩ cm resistivity) was obtained using a Direct-
8 Q system (EMD Millipore).

9 Triple-junction amorphous silicon on stainless steel substrate (SiGe-jn, Fig. S1) and carbon cloth (CC;
10 EC-CC1-060) were obtained from Xunlight Corp. and Toyo Corp., respectively.

11

12 **2. Preparation of Ru-MeCN complex**

13 The [Ru{4,4'-di(1-H-1-pyrrolyl)carbonate}-2,2'-bipyridine}(CO)₂Cl₂] (Ru-CO) complex was
14 synthesized according to a previously reported method.¹⁻³

15 A MeCN solution (200 mL) containing 137.2 mg (0.2 mmol) Ru-CO was irradiated using a white
16 fluorescent light for 15 h at room temperature. After the solvent was evaporated under reduced pressure, the
17 residual red solid was recrystallized from MeCN/ether. Yield: 89%. ¹H NMR (δ, 400 MHz, (acetone-d₆):
18 10.16 (d, 1H, *J* = 5.6 Hz, *bpy*-6'), 9.39 (d, 1H, *J* = 5.6 Hz, *bpy*-6), 9.06 (s, 1H, *bpy*-3'), 8.94 (s, 1H, *bpy*-3),
19 8.41 (d, 1H, *J* = 5.6 Hz, *bpy*-5'), 8.02 (d, 1H, *J* = 5.6 Hz, *bpy*-5), 6.78 (m, 2H, *pyrrol*), 6.02 (m, 2H, *pyrrol*),

1 4.45 (m, 2H, $-CH_2$), 4.21 (m, 2H, $-CH_2$), 2.32 (m, 2H, $-CH_2$), 2.25 (s, 3H, CH_3 -CN). FT-IR (MeCN) ν_{CO} /
2 $cm^{-1} = 1976$. m/z (ESI-MS): 722.05 $[M+Na]^+$; 713.05 $[M - MeCN+MeOH+Na]^+$.

3

4 **3. Fabrication of CC/p-RuCP by chemical polymerization of ruthenium complex**

5 Ru-MeCN (0.0179 mmol) dissolved in MeCN (5.0 mL) was polymerized using a chemical method. A 0.2
6 M $FeCl_3$ ethanol solution (0.1 mL) and 0.05 vol% pyrrole MeCN solution (0.02 mL) were used as chemical
7 polymerization initiators. The polymer solution (0.4 mL) was dropped onto the CC surface (9 cm^2) and dried
8 at 333 K for 5–10 min. The coating procedure was repeated 10 times and the resulting CC/p-RuCP was
9 placed in the dark at room temperature overnight, after which the CC/p-RuCP was rinsed with pure water.
10 The CC/p-RuCP were then cut into quarters. To fabricate the SiGe-jn/CC/p-RuCP photocathode, CC/p-
11 RuCP was connected to the stainless steel side of SiGe-jn with silver paste. The edges of the SiGe-jn/CC/p-
12 RuCP and connection points were covered with silicon rubber.

13

14 **4. Preparation of IrO_x nanocolloid solution**

15 An IrO_x nanocolloid solution was prepared according to the method reported by Zhao et al.⁴ 50 mL of 2
16 mM potassium hexachloroiridate (IV) aqueous solution was adjusted to pH 13 with 10 wt% NaOH solution
17 and heated at 383 K for 20 min. The solution was then kept in an ice bath and adjusted to pH 1 by the
18 addition of 3M nitric acid. The solution was then adjusted to pH 12 by the addition of 1.5 wt% NaOH
19 solution to yield a dark blue colored solution.

20

1 **5. Fabrication of SiGe-jn electrode**

2 The SiGe-jn was cut with scissors into rectangular plates (18 mm × 20 mm) and etched at the edges with
3 ITO etching solution. For the ITO etching process, the center of the ITO surface was masked with tape and
4 immersed in ITO etching solution for 3 h. The masking tape was then removed and the etched SiGe-jn plates
5 were rinsed with pure water and dried at room temperature. To fabricate the SiGe-jn photocathode, copper
6 tape was attached to the upper side of the ITO surface on SiGe-jn and covered with a glass substrate. The
7 copper wire was fixed on the glass substrate using indium solder and connected with copper tape onto SiGe-
8 jn. To fabricate the SiGe-jn photoanode, the stainless steel substrate of SiGe-jn was covered with a glass
9 substrate. Copper wire was fixed to the glass substrate using indium solder and connected to the stainless
10 steel using silver paste. The edges of the SiGe-jn plate and connection points were sealed with silicon rubber.

11

12 **6. Fabrication of IrO_x/SiGe-jn photoanode**

13 50 μL of IrO_x nanocolloid solution was dropped onto the ITO surface of the SiGe-jn photoanode and
14 dried at 333 K for 10 min in an oven. The ITO surface modified with IrO_x nanoparticles was then rinsed
15 with pure water to remove the salt precipitated on the surface.

16

17 **7. Fabrication of monolithic IrO_x/SiGe-jn/CC/p-RuCP device**

18 The IrO_x/SiGe-jn photoanode was broken down with a cutter knife to obtain IrO_x/SiGe-jn structure. The
19 silicon rubber and silver paste were removed from IrO_x/SiGe-jn structure. CC/p-RuCP was connected to
20 the stainless steel substrate of IrO_x/SiGe-jn with silver paste. The edges of the IrO_x/SiGe-jn/CC/p-RuCP

1 structure and connection point were sealed with silicon rubber.

2

3 **8. Electrochemical/photoelectrochemical measurements**

4 A bi-potentiostat (2325, ALS Co., Ltd.) was used for the electrochemical and photoelectrochemical
5 measurements. For typical electrochemical experiments, the sample electrode, platinum wire, and a
6 silver/silver chloride electrode (Ag/AgCl; ALS Co., Ltd.) or mercury/mercurous sulfate electrode
7 (Hg/Hg₂SO₄; ALS Co., Ltd.) were used as the working, counter, and reference electrodes, respectively. A
8 quartz cell was used as the reactor and 0.1M potassium phosphate buffer solution (K₂HPO₄:KH₂PO₄ = 1:1)
9 was used as the electrolyte. CO₂ gas was bubbled into the electrolyte for 20 min prior to the measurement
10 and allowed to flow at 20 mL min⁻¹ during the measurement. Simulated solar light was irradiated using a
11 solar simulator (HAL-320, Asahi Spectra Co., Ltd.). The intensity was adjusted at 1 sun [Air Mass 1.5
12 (AM1.5)] using a light intensity checker (CS-20, Asahi Spectra Co., Ltd.).

13

14 **9. Calculation of the potential values versus RHE**

15 The potential values expressed in the versus RHE form were obtained using the following equations.

$$16 \quad E \text{ (vs. RHE)} = E_a + 0.059 \text{ pH} + 0.199 \text{ (for Ag/AgCl)}$$

$$17 \quad E \text{ (vs. RHE)} = E_a + 0.059 \text{ pH} + 0.652 \text{ (for Hg/Hg}_2\text{SO}_4)$$

18 E_a : Applied potential

19 The pH of the phosphate buffer solution saturated with CO₂ was around pH 6.4.

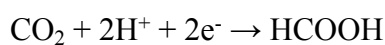
1 The CO₂ reduction potential of the ITO electrode was calculated using the following equation according to
2 the report by Z. M. Detweiler et al..⁵

$$3 \quad \text{RHE} = -1.4 + 0.059 \times 4.4 + 0.242 \text{ (for SCE)} = -0.90 \text{ V (vs. RHE)}$$

4

5 **10. Calculation of current efficiency for formate production**

6 The photoreduction of CO₂ to formate is described as:



8 The current efficiency for the production of formate was obtained using the following equation.

$$9 \quad \eta_{\text{C}} = Q_{\text{F}} \times 2 / (C/F) \times 100$$

10

11 η_{C} : Current efficiency for formate production

12 Q_{F} : Quantity of formate (mol)

13 C: Charge (C)

14 F: Faraday constant = 96485.3365 (C/mol)

15 Details of the experimental conditions are given in sections 11 and 12, Fig. S2 and in Table S1.

16

17 **11. Current efficiency for formate production as a function of oxygen concentration in CO₂ flow**

18 SiGe-jn/CC/p-RuCP or InP/RuCP photocathodes, Hg/Hg₂SO₄ and platinum wire were used as working,

19 reference and counter electrodes, respectively. A Pyrex glass cell was used as the reactor and 0.1M

1 potassium phosphate buffer solution ($K_2HPO_4:KH_2PO_4 = 1:1$) was used as the electrolyte. CO_2 gas (or CO_2
2 containing oxygen gas) was bubbled into the electrolyte for 20 min prior to the measurement and allowed to
3 flow continuously at 20 mL min^{-1} during the measurement. A xenon light source (MAX-302, Asahi Spectra
4 Co., Ltd., ca. 1 sun) equipped with an optical filter (LUX422, Asahi Spectra Co., Ltd., $\lambda > 400\text{ nm}$) and a
5 cold mirror was used to irradiate visible light. CO_2 photoreduction reaction was conducted under light
6 irradiation for 1 h at $+0.21\text{ V}$ (vs. RHE) and $+1.41\text{ V}$ (vs. RHE) for the InP/RuCP and SiGe-jn/CC/p-RuCP
7 photocathodes, respectively. The charge, amount of formate and the current efficiency for formate
8 production are shown in Table S2.

9

10 **12. Current efficiency for formate production over RuCP coated onto the stainless steel surface of the** 11 **SiGe-jn photocathode or onto the CC connected with the SiGe-jn photocathode**

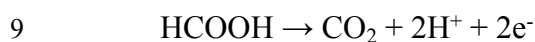
12 The SiGe-jn/RuCP photocathode, where RuCP was directly coated onto the stainless steel substrate of
13 SiGe-jn, or the SiGe-jn/carbon cloth (CC)/p-RuCP photocathode, where RuCP was coated onto the CC and
14 connected to the stainless steel substrate of SiGe-jn, were used as the working electrode of a three-electrode
15 configuration. Pt wire and Hg/Hg₂SO₄ electrode were used as the counter and reference electrodes,
16 respectively. 0.1M phosphate buffer saturated with CO_2 was used as the electrolyte. Current-time
17 measurements were conducted at $+1.41\text{ V}$ (vs. RHE) for 3 h under light irradiation. The charge, amount of
18 formate and current efficiency for the production of formate are shown in Table S3.

19

20 **13. Photodegradation of formate over IrO_x/SiGe-jn photoanode**

1 The IrO_x/SiGe-jn photoanode was used as the working electrode in a three-electrode configuration. Pt
2 wire and Ag/AgCl electrode were used as the counter and reference electrodes, respectively. 0.1M
3 potassium phosphate buffer solution (K₂HPO₄:KH₂PO₄ = 1:1) containing ca. 27 μmol of formate was used
4 as the electrolyte. Simulated solar light was irradiated using a solar simulator (HAL-320, Asahi Spectra Co.,
5 Ltd.) at an intensity of 1 sun (AM1.5). The photodegradation test was conducted at -0.25 V (vs. RHE). The
6 bias voltage was set at the operation point of the IrO_x/SiGe-jn/CC/p-RuCP device. CO₂ gas (or CO₂
7 containing oxygen gas) was continuously flowed into the reactor during the experiment.

8 The photodegradation of formate is described as:



10 An anodic charge of 4 C was observed during the photooxidation reaction over the IrO_x/SiGe-jn photoanode
11 in phosphate buffer solution containing 27 μmol of formate.

12 The amount of formate Q_F that was estimated to remain after the photodegradation reaction was calculated
13 as follows:

14
$$Q_F = 27 \text{ (}\mu\text{mol)} - (4 \text{ (C)}/96485.3365 \text{ (C/mol)}/2) \times 10^6 = \text{ca. } 6 \text{ }\mu\text{mol}$$

15 This value is shown in Fig. 1B as the calculated value. Therefore, this result indicates that formate was not
16 photodecomposed over the IrO_x/SiGe-jn photoanode, even though the observed anodic charge was sufficient
17 to decompose formate from 27 to 6 μmol.

18 The photodegradation test was also conducted under the same conditions using 0.1M potassium sulfate,
19 potassium tetraborate and potassium bicarbonate electrolytes containing formate. However, the

1 photodegradation of formate was also negligible in the sulfate, borate and carbonate electrolytes. The results
2 for the photodegradation of formate are shown in Figs. 1B and S5.

3

4 **14. CO₂ photoreduction reaction using tablet-formed IrO_x/SiGe-jn/CC/p-RuCP device**

5 A quartz cell was used as the reactor and 0.1M potassium phosphate buffer solution (K₂HPO₄:KH₂PO₄ =
6 1:1) was used as the electrolyte. The tablet-formed IrO_x/SiGe-jn/CC/p-RuCP device was immersed in the
7 electrolyte solution and CO₂ gas was bubbled into the reactor for 20 min prior to the measurement and
8 allowed to flow at 20 mL min⁻¹ during the measurement. A solar simulator (HAL-320, Asahi Spectra Co.,
9 Ltd.) was used as the light source for irradiation from the IrO_x side through a 0.25 cm² square-shaped slit to
10 regulate the irradiation area, with the intensity at 1 sun (AM 1.5) on the surface of the device, as measured
11 using a light intensity checker (CS-20, Asahi Spectra Co., Ltd.).

12

13 **15. Determination of products in the aqueous phase**

14 The amount of HCOO⁻ was determined using an ion chromatograph (ICS-2000, Dionex Corporation) with
15 IonPacAS15 and IonPacAG15 columns and a conductometric detector. The column temperature was
16 maintained at 308 K. A 3 mM KOH solution was used as the first eluent for 10 min. The eluent was then
17 gradually changed to 10 mM KOH for the next 5 min, after which the eluent was gradually changed to 60
18 mM KOH for the next 10 min.

19 The calibration curve was obtained using HCOOH solutions prepared at different concentrations (0.01,
20 0.05, 0.1, 0.2, and 0.5 mM) by dilution with pure water. The calibration curve was measured prior to every

1 experiment. The calibration curve was checked using HCOOH solutions prepared by diluting HCOOH with
2 the potassium phosphate buffer solution used as electrolyte. The calibration curve was identical for both
3 cases And the accuracy of the measurement was $\pm 5\%$.

4 To detect the formation of $\text{H}^{13}\text{COO}^-$, an ion chromatograph interfaced with a time-of-flight mass
5 spectrometry system (IC-TOFMS, Jeol JMS-T100LP) was used with MeOH as the mobile phase.

6

7 **16. Determination of products in the gas phase**

8 The amount of oxygen and hydrogen in the gas phase were determined by *in situ* measurements using a
9 flow reactor combined with a gas chromatograph. The flow reactor (Makuhari Rikagaku Garasu Inc.) was
10 equipped with an auto sampler for *in situ* measurements and was directly connected to the gas
11 chromatograph (GC-2014, Shimadzu Corporation) equipped with Porapak-N and MS-13X columns. The
12 calibration was conducted using CO_2 -based standard gas containing 100 ppm H_2 , N_2 , O_2 , CO , and
13 hydrocarbons.

14 At the start of the experiment, the CO_2 gas flow was 20 mL min^{-1} for 2 h to remove air in the reactor. CO_2
15 photoreduction was then conducted with a continuous CO_2 flow of 20 mL min^{-1} . A solar simulator (HAL-
16 320, Asahi Spectra Co., Ltd.) equipped with an optical fiber and rod lens was used as a light source. The
17 light irradiation area was increased to ca. 1 cm^2 to obtain a large amount of gaseous products for more
18 accurate determination. However, it was difficult to maintain sufficient distance to obtain a uniform light
19 irradiation area due to the experimental space and the shape of the irradiation area was obtained as some
20 spots which caused by the lens array structure of collimator lens in the rod lens. Therefore, the light intensity

1 could not be correctly adjusted to 1 sun (AM1.5, 0.25 cm²). More than 100 ppm of gaseous product is
2 preferable for accurate determination (accuracy ±3%) in this system and 250–300 ppm of gaseous oxygen
3 was detected under the experimental conditions.

4

5 **17. Calculation of solar-to-chemical conversion efficiency for formate production**

6 The efficiency for formate production was calculated using the following equation:

$$7 \quad \text{SCE} = (R_F \times \Delta G) / (I \times A) \times 100$$

8 SCE: Solar-to-chemical conversion efficiency (%)

9 R_F: Mean rate of formate produced (15.335 μmol/h)

10 ΔG: Change in Gibbs free energy per mole of formic acid produced from CO₂ and water (ΔG = 270

11 kJ/mol at 298 K)

12 I: Light intensity (100 mW/cm²)

13 A: Irradiation area (0.25 cm²)

14 The mean rate of formate produced was determined by the slope of the fitted line for the formate production

15 plots over a period of 6 hours, as shown in Fig. 2B.

16 Numerator:

$$17 \quad R_F \times \Delta G = 15.335 \mu\text{mol/h} \times 270 \text{ kJ/mol}$$

$$18 \quad = 15.335 / 3600 \mu\text{mol/s} \times 270 \text{ kJ/mol}$$

$$19 \quad = 1.150 \text{ mJ/s}$$

$$20 \quad = 1.150 \text{ mW}$$

1

2 Denominator:

3 $I \times A = 100 \text{ mW/cm}^2 \times 0.25 \text{ cm}^2$

4 $= 25 \text{ mW}$

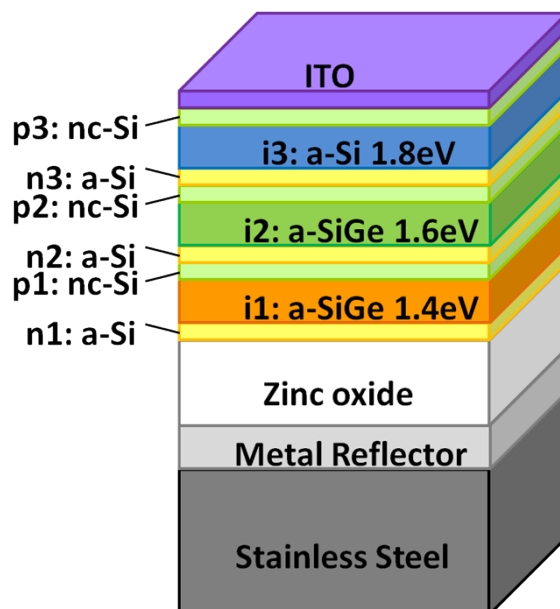
5

6 $\text{SCE} = 1.150 / 25 \times 100 = 4.6\%$

7

8 **18. References**

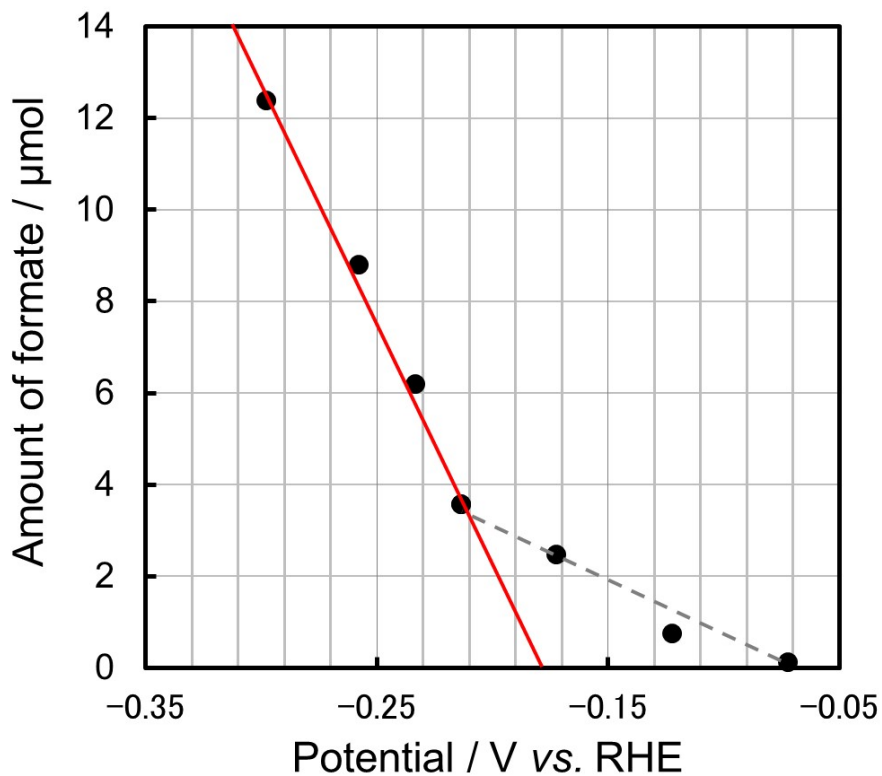
- 9 1. M. N. Collomb-Dunand-Sauthier et al., *J. Phys. Chem.*, **1993**, 97, 5973-5979.
- 10 2. M. N. Collomb-Dunand-Sauthier et al., *J. Organometal. Chem.*, **1993**, 444, 191-198.
- 11 3. P. A. Anderson et al., *Inorg. Chem.*, **1995**, 34, 6145- 6157.
- 12 4. Y. Zhao et al., *J. Phys. Chem. Lett.*, **2011**, 2, 402-406.
- 13 5. Z. M. Detweiler, et al, *Langmuir*, **2014**, 30, 7593-7600.



1

2

3 **Figure S1.** Schematic illustration of the SiGe-jn structure. Amorphous Si (a-Si) is irradiated with light
 4 from the ITO side. The direction of flow of photoexcited electrons is from the ITO side to the stainless steel
 5 side. Therefore, CO₂ reduction occurs at the stainless steel side and H₂O oxidation occurs at the ITO side.



1

2

3 **Figure S2.** Relation between applied potential and amount of formate generated over the CC/p-RuCP

4 photocathode. The CC/p-RuCP photocathode was used as the working electrode of a three-electrode

5 configuration. Pt wire and a Hg/Hg₂SO₄ electrode were used as the counter and reference electrodes,

6 respectively. 0.1M phosphate buffer saturated with CO₂ was used as the electrolyte. CO₂ reduction reaction

7 was conducted at various applied potential from -0.07 to -0.30 V (vs. RHE). The amount of formate

8 generated during reaction for 1 h is plotted. The CO₂ reduction potential over CC/p-RuCP was evaluated to

9 be approximately -0.18 V (vs. RHE) from the intercept with the x-axis and the steeper slope observed from -

10 0.21 to -0.30 V (vs. RHE). The charge, amount of formate and current efficiency observed for CC/p-RuCP

11 cathode at various applied potentials are shown in Table S1.

12

13

Applied potential (V vs. RHE)	Charge (C)	Formate (μmol)	Current efficiency (%)
-0.07	0.03	0.13	78
-0.12	0.19	0.75	78
-0.17	0.59	2.48	81
-0.21	0.82	3.57	84
-0.23	1.39	6.20	86
-0.26	1.92	8.81	89
-0.30	2.87	12.4	83

1

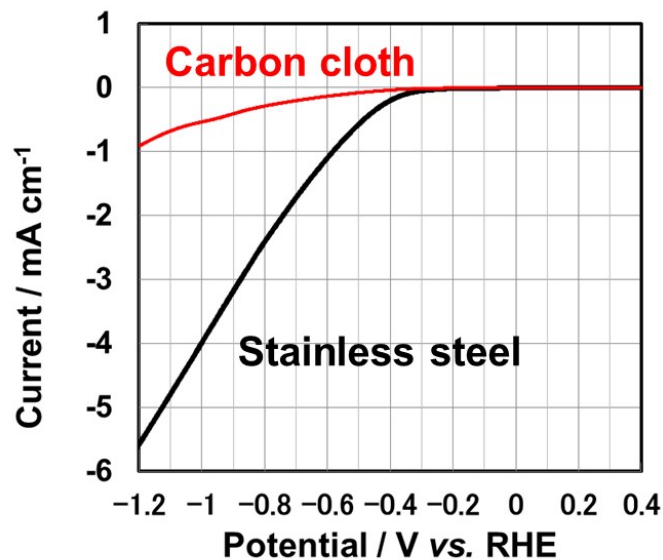
2

3 **Table S1.** Current efficiency for formate production over CC/p-RuCP cathode at various applied
4 potentials. The current efficiency for formate production on the SiGe-jn/CC/p-RuCP photocathode was
5 better than that for CC/p-RuCP. However, it is difficult to determine the CO₂ reduction potential over p-
6 RuCP using the SiGe-jn/CC/p-RuCP photocathode; therefore, a CC/p-RuCP cathode was used as a working
7 electrode for the three-electrode configuration.

8

Cathode	Applied potential (V vs. RHE)	Oxygen Concentration (%)	Charge (C)	Formate (μmol)	Current efficiency (%)
InP/RuCP	+0.21	0	0.11	0.55	93
		2.3	0.20	0.36	35
		3.4	0.15	0.23	30
		7.2	0.12	0.04	6
SiGe-jn/CC/p-RuCP	+1.41	0	5.18	25.2	94
		2.3	5.44	24.8	88
		3.4	5.62	25.6	88
		7.2	5.32	20.6	75

Table S2. Current efficiency for formate production with respect to the oxygen concentration in the CO_2 flow over SiGe-jn/CC/p-RuCP and InP/RuCP photocathodes under light irradiation for 1 h in 0.1M phosphate buffer electrolyte. SiGe-jn/CC/p-RuCP or InP/RuCP photocathodes, Hg/Hg₂SO₄ and platinum wire were used as working, reference and counter electrodes, respectively. A Pyrex glass cell was used as the reactor and 0.1 M potassium phosphate buffer solution (K₂HPO₄:KH₂PO₄ = 1:1) was used as the electrolyte. CO₂ gas (or CO₂ containing oxygen gas) was bubbled into the electrolyte for 20 min prior to the measurement and allowed to flow continuously at 20 mL min⁻¹ during the measurement. A xenon light source (MAX-302, Asahi Spectra Co., Ltd., ca. 1 sun) equipped with an optical filter (LUX422, Asahi Spectra Co., Ltd., $\lambda > 400$ nm) and a cold mirror was used to irradiate visible light. CO₂ photoreduction reaction was conducted under light irradiation for 1 h at +0.21 V (vs. RHE) and +1.41 V (vs. RHE) for the InP/RuCP and SiGe-jn/CC/p-RuCP photocathodes, respectively.



1

2

3 **Figure S3.** Current-potential characteristics of CC and stainless steel substrates for SiGe-jn. The CC

4 electrode and stainless steel substrate of SiGe-jn were used as the working electrode for a three-electrode

5 configuration. Pt wire and Ag/AgCl electrode were used as the counter and reference electrodes,

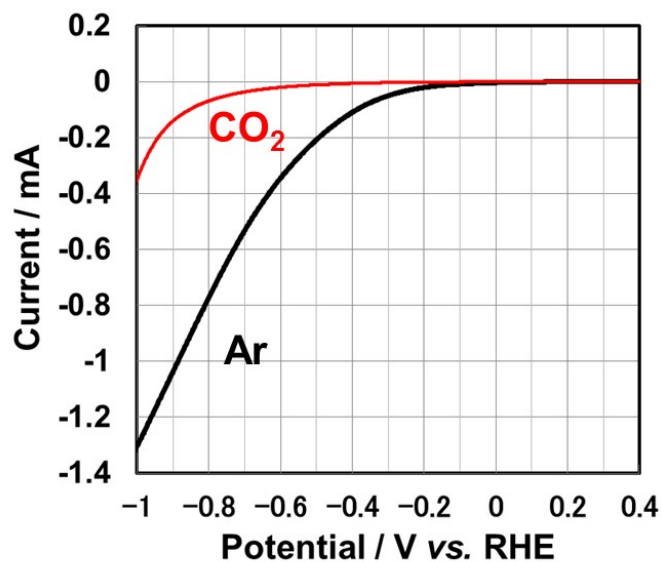
6 respectively. 0.1M phosphate buffer saturated with CO₂ was used as the electrolyte. The scan rate was 50

7 mV/s and the scan direction was negative. The current axis is displayed as anodic positive. Stainless steel

8 showed a high cathodic current compared with CC. Many bubbles of hydrogen were observed over the

9 stainless steel substrate, while a negligible amount of bubbles was generated over CC, which suggests

10 preferential hydrogen generation over stainless steel.



1

2

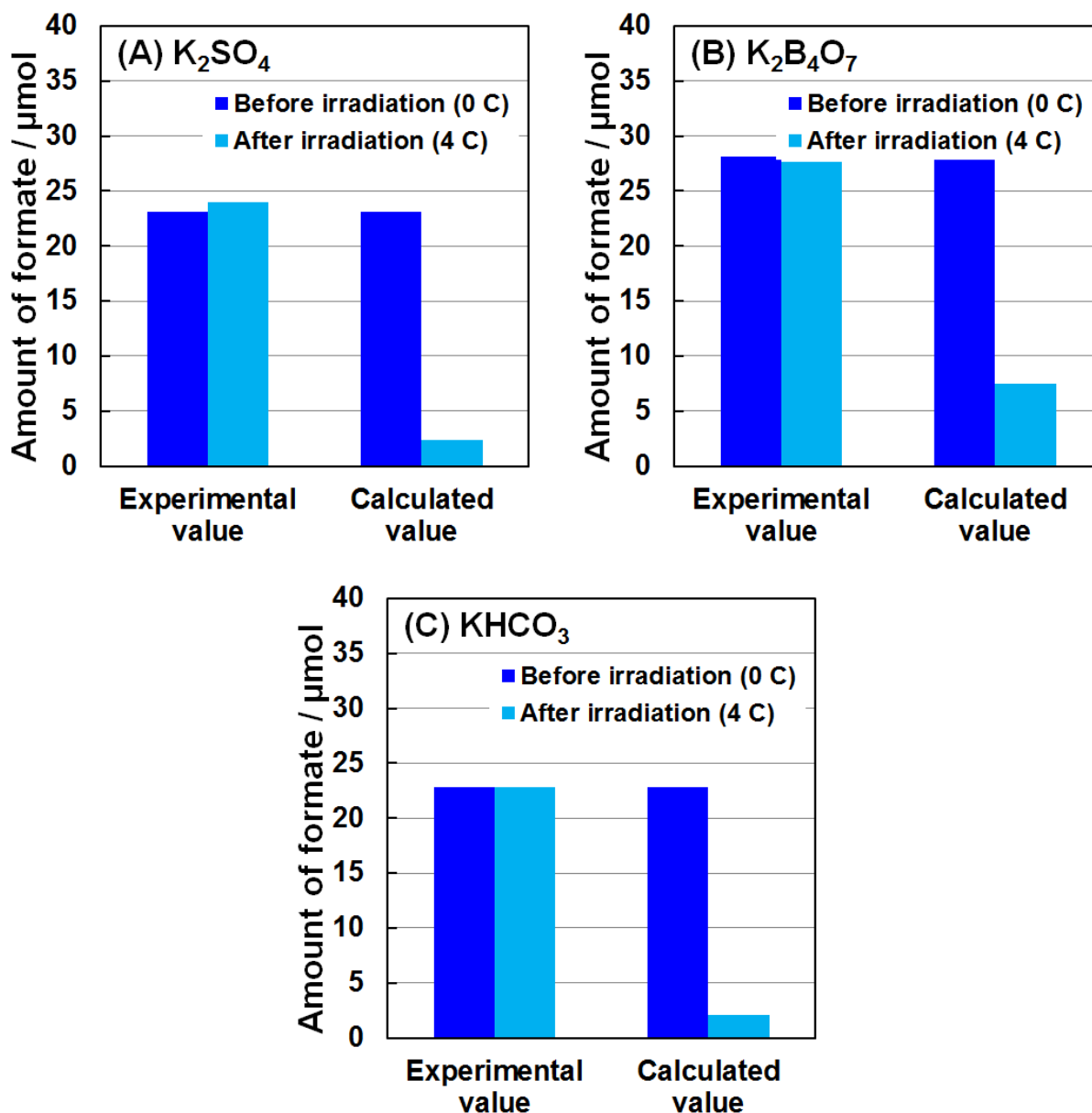
3 **Figure S4.** Current-potential characteristics of CC under Ar or CO₂ atmospheres. The CC electrode
4 was used as the working electrode of a three-electrode configuration. Pt wire and Hg/Hg₂SO₄ electrode were
5 used as the counter and reference electrodes, respectively. 0.1M phosphate buffer was used as the electrolyte.
6 The scan rate was 100 mV/s and the scan direction was negative. CC under a CO₂ atmosphere showed a low
7 cathodic current compared with that under an Ar atmosphere. This result indicates that CO₂ adsorbed on the
8 surface of CC and the accessibility of protons to CC was prevented by the presence of CO₂.

Substrate	Charge (C)	Formate (μmol)	Current efficiency (%)
Stainless steel	13.3	0.2	0.3
Carbon cloth	18.4	89.6	94

1

2

3 **Table S3** Current efficiency for formate production over RuCP coated onto the stainless steel surface
4 of the SiGe-jn photocathode or onto the CC connected with the SiGe-jn photocathode. The SiGe-jn/RuCP or
5 SiGe-jn/CC/p-RuCP photocathodes were used as the working electrode of the three-electrode configuration.
6 Pt wire and Hg/Hg₂SO₄ electrodes were used as the counter and reference electrodes, respectively. 0.1M
7 phosphate buffer saturated with CO₂ was used as the electrolyte. Current-time measurements were
8 conducted at +1.41 V (vs. RHE) for 3 h under light irradiation.



1

2

3

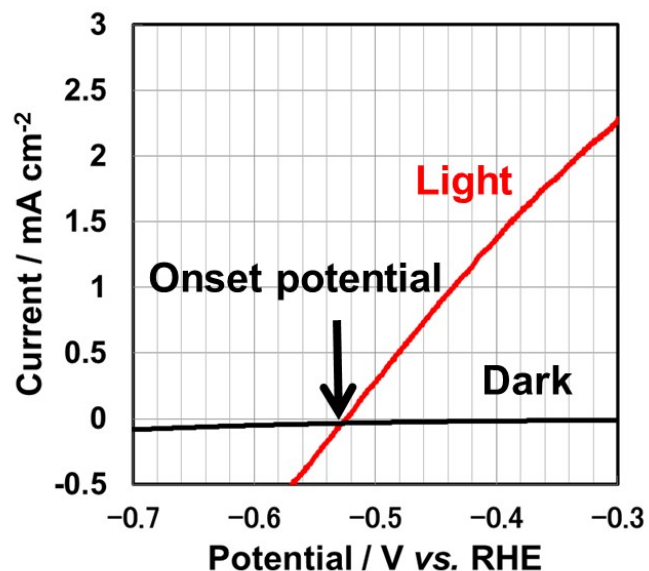
4 **Figure S5.** Amount of formate observed before and after the photodegradation test over $\text{IrO}_x/\text{SiGe-jn}$

5 photoanode in various electrolytes. Photodegradation over the $\text{IrO}_x/\text{SiGe-jn}$ photoanode was conducted at -

6 0.25 V (vs. RHE) in 0.1M of (A) potassium sulfate, (B) potassium tetraborate and (C) potassium bicarbonate

7 electrolytes. The photodegradation of formate in all electrolytes was negligible, similar to that in the

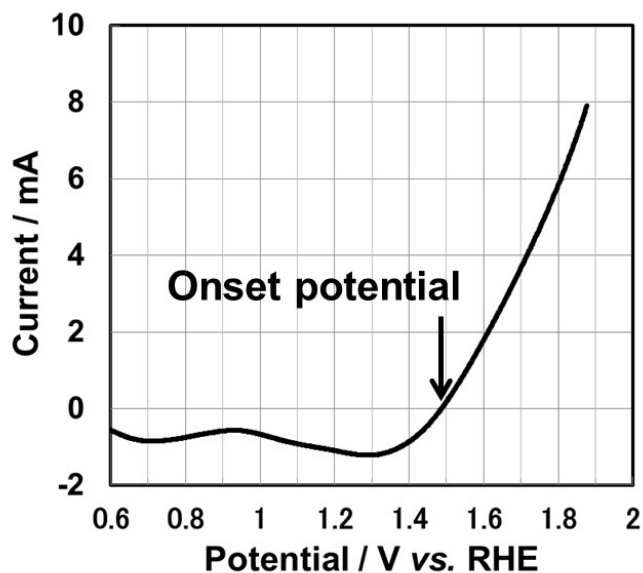
8 phosphate electrolyte.



1

2

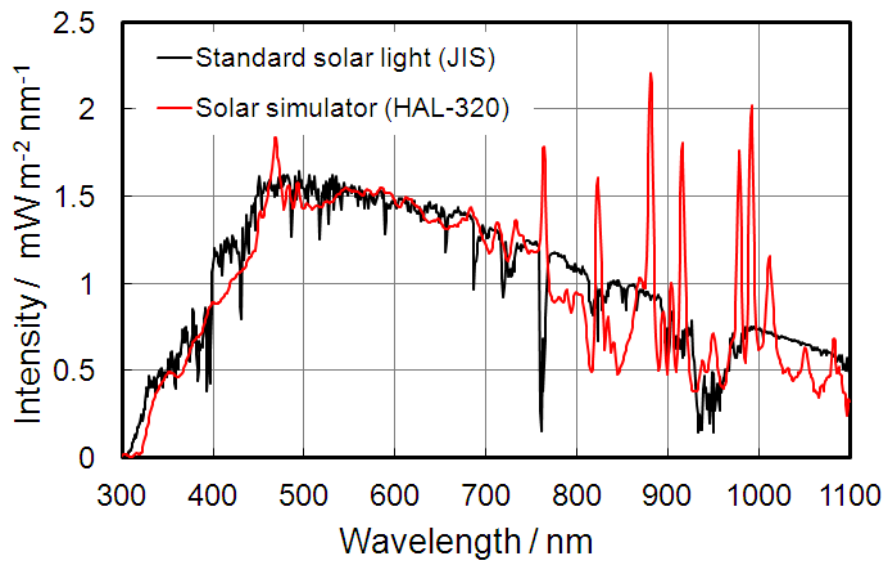
3 **Figure S6.** Current-potential characteristics for the IrO_x/SiGe-jn photoanode used as the working
4 electrode of a three-electrode configuration. Pt wire and Ag/AgCl electrode were used as the counter and
5 reference electrodes, respectively. 0.1M phosphate buffer saturated with CO₂ was used as the electrolyte.
6 Simulated solar light (1 sun, AM1.5) was irradiated from the IrO_x side. The scan rate was 100 mV/s and the
7 scan direction was negative. The current axis is displayed as anodic positive. The onset potential was
8 estimated to be -0.52 V (vs. RHE).



1

2

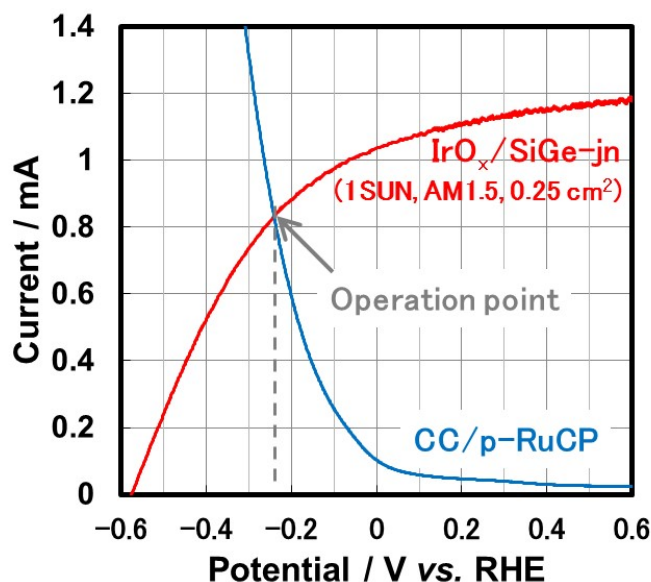
3 **Figure S7.** Current-potential characteristics for the IrO_x/ITO anode used as the working electrode of a
4 three-electrode configuration. Pt wire and Ag/AgCl electrode were used as counter and reference electrodes,
5 respectively. 0.1M phosphate buffer was used as the electrolyte. The scan rate was 100 mV/s and the scan
6 direction was negative. The current axis is displayed as anodic positive. The onset potential of water
7 oxidation reaction over the IrO_x/ITO electrode was estimated to be +1.5 V (vs. RHE).



1

2

3 **Figure S8.** Spectrum of simulated solar light provided by Asahi Spectra Co., Ltd. Japanese industrial
4 standards (JIS C8904-3 (2011)) is equivalent to International Electrotechnical Commission (IEC).



1

2

3 **Figure S9.** Current-potential characteristics for the IrO_x/SiGe-jn photoanode and CC/p-RuCP cathode.

4 The IrO_x/SiGe-jn photoanode and CC/p-RuCP cathode were used as working electrodes in a three-electrode

5 configuration, where Pt wire and Ag/AgCl electrodes were used as the counter and reference electrodes,

6 respectively. 0.1M phosphate buffer saturated with CO₂ was used as the electrolyte. The scan rate was 100

7 mV/s and the scan direction was negative. The photocurrent of 3.3 mA/cm² was observed at the operation

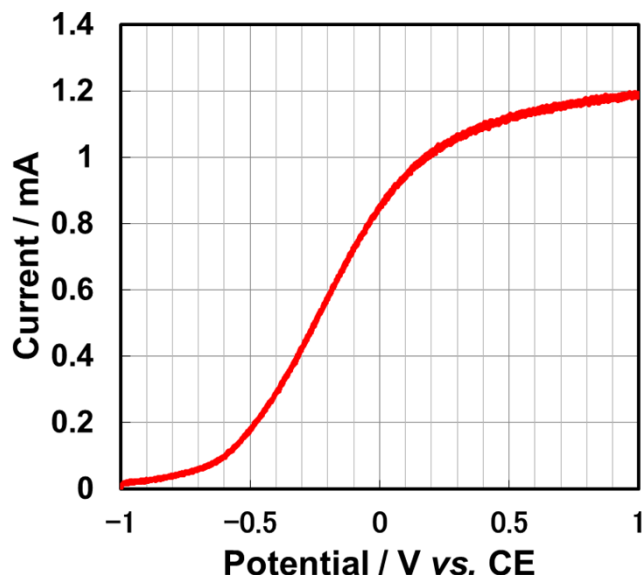
8 point, which corresponds to a solar-to-chemical energy conversion efficiency of 4.3%, considering the

9 current efficiency for formate production of 94%. The current axis is displayed as anodic positive for the

10 IrO_x/SiGe-jn photoanode and cathodic positive for the CC/p-RuCP cathode. The operation point was

11 estimated to be -0.24 V (vs. RHE), which approximately corresponds to that observed in the two-electrode

12 configuration (Fig. S9).



1

2

3 **Figure S10.** Current-potential characteristics for the IrO_x/SiGe-jn photoanode and CC/p-RuCP cathode

4 in a two-electrode configuration under simulated solar light irradiation (1 sun, AM1.5, 0.25 cm²). 0.1M

5 phosphate buffer saturated with CO₂ was used as the electrolyte. The scan rate was 100 mV/s and the scan

6 direction was positive. The photocurrent of 3.4 mA/cm² was observed at 0 V (vs. counter electrode (CE)),

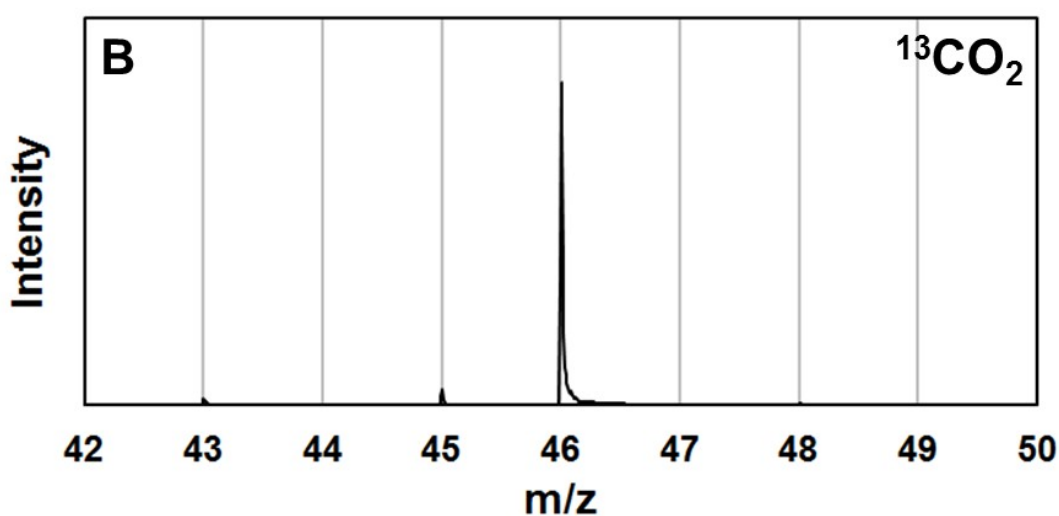
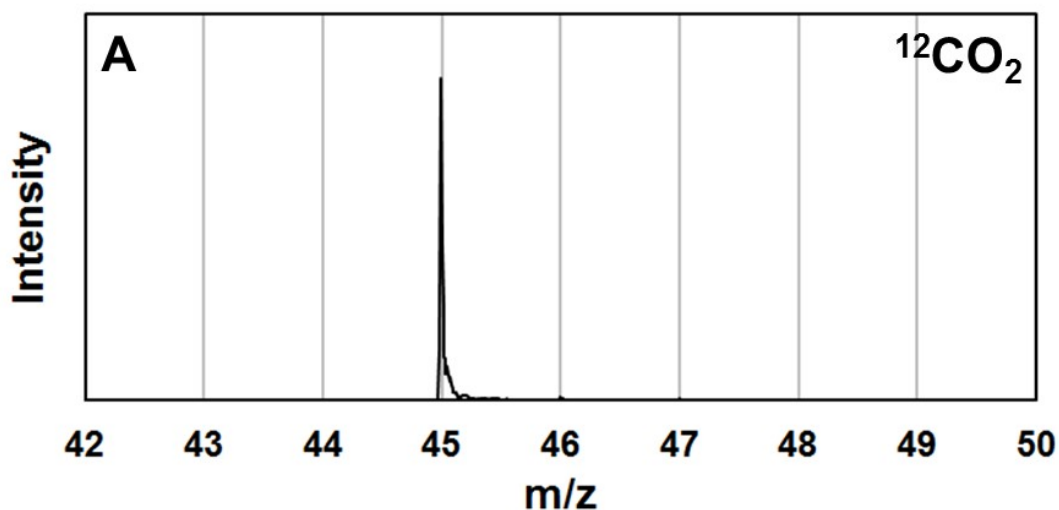
7 which corresponds to a solar-to-chemical energy conversion efficiency of 4.5%, considering the current

8 efficiency for formate production of 94%. The efficiency approximately corresponds to that observed in the

9 IrO_x/SiGe-jn/CC/p-RuCP device. The operation point was determined to be -0.25 V (vs. RHE) by voltage

10 measurement between the Ag/AgCl electrode and the IrO_x/SiGe-jn photoanode in the two-electrode

11 configuration with the CC/p-RuCP cathode.



1

2

3

4 **Figure S11.** Mass spectra for the products observed in the CO_2 photoreduction reaction under $^{12}\text{CO}_2$
 5 (A) and $^{13}\text{CO}_2$ (B) atmospheres. The spectra were measured at the peak observed at 8 minutes in ion
 6 chromatograph measurement (The IC-MS spectrum for $m/z = 46$ is shown in Fig. 3B). The spectrum
 7 observed under $^{12}\text{CO}_2$ (A) corresponded to the calculated isotopic distribution of HCOO^- . The main peak in
 8 the spectrum under $^{12}\text{CO}_2$ ($m/z = 45$) was shifted to $m/z = 46$ under the $^{13}\text{CO}_2$ atmosphere, which indicates
 9 that formate was produced by the photoreduction of CO_2 .

10